RSCF: Relation-Semantics Consistent Filter for Entity Embedding of Knowledge Graph

Anonymous ACL submission

Abstract

In knowledge graph embedding, leveraging relation-specific entity-transformation has markedly enhanced performance. However, this approach lacks assurance for consistent changes in relation and entity embeddings due to the disconnected entity-transformation representation, missing valuable inductive bias among semantically similar relations. Furthermore, a generalized plug-in approach as a SFBR disrupts this consistency through excessive concentration of entity embeddings under entity-based regularization, generating indistinguishable score distributions among relations. To tackle these challenges, we introduce *Relation-Semantics Consistent Filter* (RSCF), characterized by three features: 1) shared affine transformation of relation embeddings across all relations, 2) change-based entity-transformation that adds an entity embedding to its change represented by the transformed vector, and 3) normalization of the change to prevent scale reduction. In knowledge graph completion tasks with distance-based and tensor decomposition models, RSCF notably enhances performance across all relations, particularly in rare relations in long-tailed distribution.

1 Introduction

Knowledge graphs (KGs) play crucial roles in a wide area of machine learning and its applications (Liu et al., 2021; Zhang et al., 2022b; Zhou et al., 2022; Fang et al., 2017; Gao et al., 2019; Cao et al., 2019; Geng et al., 2022; Wang et al., 2019). The KGs, even on a large scale, still suffer from a lack of data. For example, 71% of people in Freebase have no birthplace information, and 75% have no nationality information (Dong et al., 2014). This incompleteness issue has been extensively studied as a task to predict missing entity information, called as knowledge graph completion (KGC). An effective approach for KGC is knowledge graph embedding (KGE) that learns vectors to represent entities and relations in a low dimensional space to measure the validity of triples. Two primary approaches to determine the validity are distance-based model (DBM) using the Minkowski distance and tensor decomposition model (TDM) regarding KGC as a tensor completion problem (Zhang et al., 2020b). A recently tackled issue of the models is to learn only single embedding for an entity, which is insufficient to express its various attributes in complex relation patterns such as 1-N, N-1 and N-N (Wang et al., 2014; Chao et al., 2021; Ge et al., 2023). A proposed and effective approach for this issue is entity-transformation based model (ETM) that uses relation-specific transformations to generate different entity embeddings for relations from their original embedding, enabling more complex entity and relation learning (Liang et al., 2021; Wang et al., 2014; Chao et al., 2021; Ge et al., 2023).

ETMs, however, have a limit to learning useful inductive bias that could be obtained in semantically similar relations. For example, Semantic Filter Based on Relations (SFBR), a recently proposed method plugged in to various KGE models (Liang et al., 2021), assigns mutually disconnected relation-specific transformation to each relation. Furthermore, under a significantly useful regularizer such as DURA (Zhang et al., 2020b) and N3 (Lacroix et al., 2018), especially on TDM, the method critically concentrates entity embeddings including unobserved entities and generates indistinguishable score distributions across relations. Both issues are interpreted as limited learning an important and implicit inductive bias that semantically similar relation embeddings have similar relation-specific entity-transformation, called *relation-semantics consistency* in this paper.

To alleviate the issues, we present *Relation-Semantically Consistent Filter* (RSCF), incorporating three features: 1) shared affine transfor-

mation for consistency mapping of relations to entity-transformations, 2) change-based entity-transformation representation using the affine transformation to generate only the change of an entity-embedding subsequently added by this embedding and 3) normalization of the change for preventing critical scale reduction breaking consistency. Our contributions are as follows.

- We raise and clarify two problems of entity-transformation models in learning inductive bias in terms of *relation-semantics consistency*.
- We propose a novel and significantly outperforming relation-semantics consistent filter (RSCF) to induce the consistency as a plug-in method to KGE models.
- We provide experimental results on common benchmarks of KGC, and in-depth analysis to verify the causes and derived effects.

2 Loss of Useful Inductive Bias

Because semantically similar relations have similar embedding (Yang et al., 2014), we define that mapping relation embeddings to entity-transformations is *relation-semantically consistent* if and only if any relation pairs (r_1, r_2) and shorter pair (r_1, r_3) for a given r_1 are mapped to entity-transformation pair (T_1, T_2) and shorter pair (T_1, T_3), respectively. This consistency serves as an inductive bias implying that semantically similar relations have similar entity-transformations and, therefore, overall similar entity embeddings. Two phenomena of losing this inductive bias and their causes are as follows.

Disconnection of Entity-Transformations Disconnected entity-transforamtions loosely use this bias, especially under lack of triplet data. In existing methods, relation-specific entity-transformations use separate parameters such as $\mathsf{h}_r = \mathsf{W}_r\mathsf{h}$ and $\mathsf{t}_r = \mathsf{W}_r\mathsf{t}$ (Liang et al., 2021), where h, t, are head and tail entity embedding, and W_r is a relation-specific transformation. Despite the disconnection, the methods can still learn similar W_r for given two similar relation embeddings if their desirable entity ranks are similar. However, limited observation of entities due to sparse triplet data introduces a wide variety of possible entity-transformations and their corresponding embedding distributions, thereby diluting consistency. In this environment, the disconnected representation without any specific training and initialization process aiming to foster the consistency is exposed to the loss of useful inductive bias of similar relations.

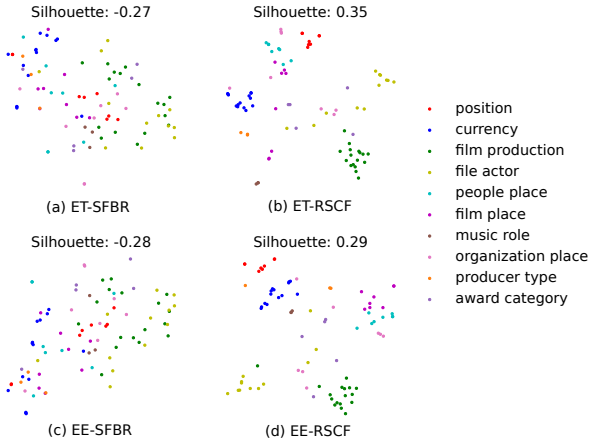

Figure 1: Head entity-transformations and entity embeddings for semantically similar relation groups. (a) and (b) indicate ET of SFBR and RSCF, (c) and (d) indicate EE of SFBR and RSCF. Points in the same color are relations in the same group. Clearly distinct Groups are selected from the original TransE (Appendix B). Silhouette score shows numerical results of their in-cluster concentration relative to inter-cluster distance.

Empirical Evidence for Disconnection Figure 1 shows the impact of the disconnection via T-SNE visualization of head entity-transformations (ET) and corresponding entity embeddings (EE) of SFBR and RSCF. We split them into relation groups, defined for clearly clustered relations in original TransE[1]. An entity for EE is randomly selected on FB15k-237. The ET and EE distribution of SFBR are mostly dispersed and overlapping between semantically different relation groups, which implies the limit in inducting relation-semantics consistency, while RSCF methods show more in-cluster concentration and decoupling clusters. The higher silhouette score of RSCF supports this phenomenon. See more detailed distributions in Appendix I.

Entity Embedding Concentration In particular, SFBR additionally loses consistency under entity-based regularization, DURA (Zhang et al., 2020b). In KGE based on tensor decomposition model, DURA has shown significant improvement enough to be inevitable. However, SFBR with DURA reduces the scale of ET, causing a strong concentra-

[1]For details about the relation group, please refer to the Appendix H.

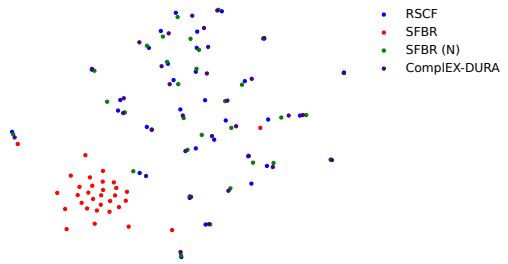

(a) Entity Embedding

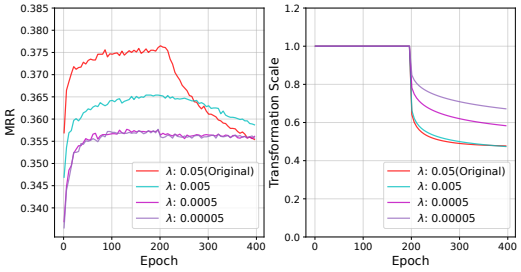

(b) Test Performance (left) and Scale (right)

Figure 2: Entity embedding concentration, and scale and performance decrease in training. The results are collected from ComplEX with DURA regularization and SFBR is applied after 200 epochs (λ: regularization weight).

tion of entire entity embeddings. Observed entities are relatively safe because the score distribution is continuously adjusted to predict correct triples, but unobserved entities are critically vulnerable to the concentration causing indistinguishable score distributions for semantically different relations, implying critically broken consistency. This cause of this phenomenon is simply derived in the following equations of DURA in the original (above) (Zhang et al., 2020b) and DURA in SFBR (below).

$$\begin{array}{ll} \sum_p & ||\mathbf{h_i}\overline{\mathbf{R_j}}||_2^2+||\mathbf{h_i}||_2^2+||\mathbf{t_k}||_2^2+||\mathbf{t_k}\overline{\mathbf{R_j}}^\top||_2^2 \\ \sum_p & ||\mathbf{W_{r_j}}\mathbf{h_i}\overline{\mathbf{R_j}}||_2^2+||\mathbf{W}_{r_j}\mathbf{h_i}||_2^2+||\mathbf{t_k}||_2^2+||\mathbf{t_k}\overline{\mathbf{R_j}}^\top||_2^2 \end{array} \quad (1)$$

where $p = (h_i, r_j, t_k) \in S$ for total training data S, $\mathbf{h_i}$ and $\mathbf{t_k}$ are head and tail embeddings with indices and $\overline{\mathbf{R_j}}$ is a matrix representing relation r_j. In the equations, the minimum scale of ET $\mathbf{W_{r_j}}$ is an optimum for distinguished regularization loss terms. Therefore, ET scales gradually decrease and end up with indistinguishable score distribution in all score distributions.

Empirical Evidence for Concentration Figure 2 presents T-SNE visualization of score distributions for selected queries. We select the relation r_1 showing significantly low performance in ComplEX-SFBR on FB15k-237, and select all queries (h, r_1, ?) for the relation r_1 in the validation set. We then generate score distribution for each query using RSCF, SFBR, SFBR with normalization (SFBR (N)), and the ComplEX-DURA. The results show that SFBR concentrates embeddings into a small and clear cluster, while the other methods are diversely dispersed.

Do We Need to Use DURA regularizer? Generating indistinguishable score distributions cannot be merely resolved by handling the regularization weight. Figure 2 (b) shows the MRR (left) of ComplEX-SFBR with DURA and transformation scale (right). In training until 200 epochs, largely weighted DURA shows significant performance, but applying SFBR starts to decrease MRR and the transformation scale. The results imply that integrating SFBR with DURA causes performance degradation with scale decrease ending up in the entity embedding concentration. However, the result of SFBR with a small weighted DURA indicates that simply excluding DURA on the tensor decomposition model will critically decrease the performance.

3 Method

Overview In this section, we propose *Relation-Semantics Consistent Filter* (RSCF) to address the consistency issues. In Figure 3, the overall filtering process of RSCF, distinguished features compared to SFBR, and their intended effects are illustrated. RSCF represents the ET as an addition of original embedding and its relation-specific change (ⓒ). The change is generated by an affine transformation from relation embedding (ⓐ), and then normalized (ⓑ), described as

$$\mathbf{e_r} = \underbrace{(\overbrace{\mathrm{N}_p}^{\text{ⓑ}}(\overbrace{\mathbf{rA}}^{\text{ⓐ}}) + \mathbf{1})}_{\text{ⓒ}} \otimes \mathbf{e} \quad (2)$$

where $\mathbf{A} \in \mathbf{R}^{n\times n}$ is shared affine transformation, $\mathbf{r}$ and $\mathbf{e} \in \mathbf{R}^n$ are relation and entity embedding. $\mathrm{N}_p(\mathbf{rA}) = \frac{\mathbf{rA}}{\|\mathbf{rA}\|_p}$, and $\otimes$ is an elementwise product. Detailed motivation and effects are as follows.

Shared Affine Transformation for Consistency Affine transformation maintains the parallelism of two parallel line segments after the transformation and preserves the ratio of their lengths. This property guarantees consistent mapping of relation

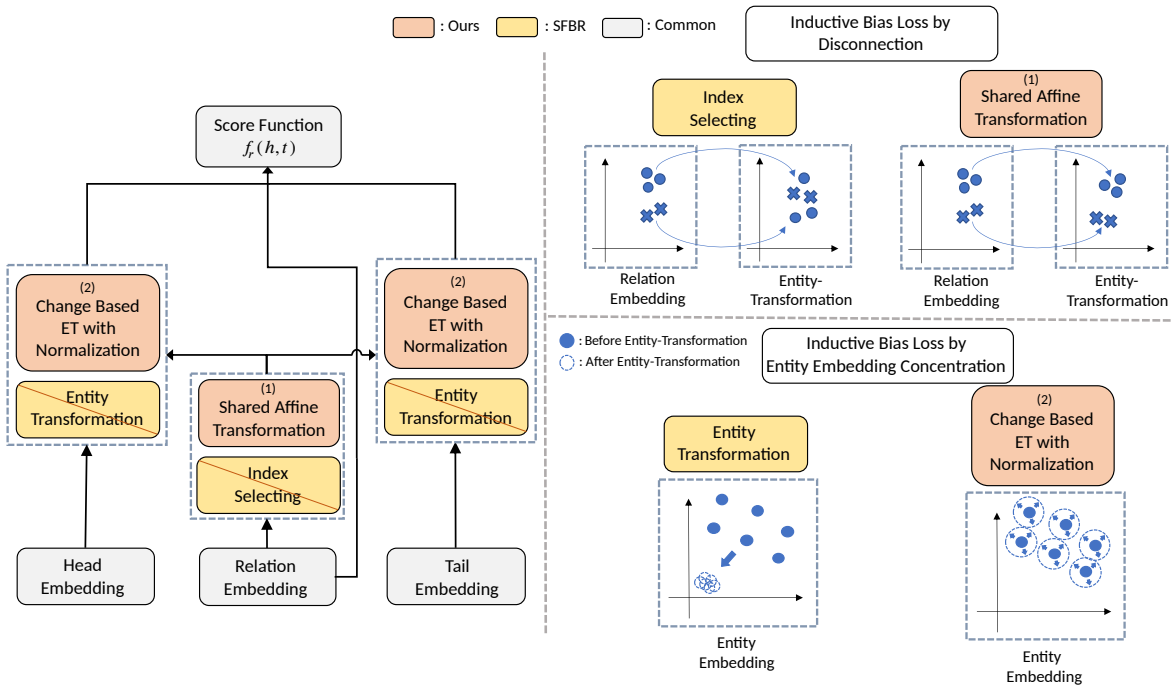

Figure 3: Overview of Relation-Semantics Consistent Filter and Its Effect. Its process (left) is illustrated on SFBR coloring changed modules. The two effects (right) are shown by comparing SFBR and RSCF on ET and entity embeddings.

embeddings at least on a line to generated vectors (part ⓐ in Equation 2). After normalization of the generated vectors (part ⓑ), the consistency still holds because the monotonic increase of distance between pairs is guaranteed even if the rate of lengths is not equally maintained (simple proof in Appendix C). The addition of one vector to the normalized change (part ⓒ) does not alter the inequality of distances of lines, so the consistency is again maintained. Overall, by applying the affine transformation, we can maintain the consistency between relation embedding and its ET. To implement the affine transformation shared across relations, we simply adopt a linear transformation for $\mathbf{A}$.

Change Based Entity Transformation Sharing an affine transformation over all relations inevitably reduces the expressiveness of ET compared to entirely separate relation-specific transformations such as SFBR that has shown to yield positive results (Liang et al., 2021). To mitigate the negative effects from this reduction, we decrease required expressiveness by learning only the changes in entity embeddings, rather than learning their diverse positions. Moreover, this change-based ET representation enables safely bounding changes via normalization without altering original entity embeddings. To implement it, we add one to the normalized change $\mathbf{N}_p(\mathbf{rA})$ and multiply it to the original entity-embedding (part ⓒ).

Normalization of Change for Reducing Entity Embedding Concentration The change generated from the affine transformation is normalized by its length, expressed as $\mathbf{N}_p(\mathbf{rA})$ in the part ⓑ. This normalization alleviates critical entity embedding concentration via reducing scale decrease of transformed entity embeddings $\mathbf{e_r}$ in DURA regularization. In our relation-specific change based ET, the change of $\mathbf{e_r}$ is simply written as

$$\|\alpha \otimes \mathbf{e}\|_p \tag{3}$$

where $\alpha = \mathbf{N}_p(\mathbf{rA})$. This value has a maximum when α has the same direction to $\mathbf{e}$. Since α is a unit vector in p-norm, $\alpha = \mathbf{e}/\|\mathbf{e}\|_p$. Then, the maximum change is

$$\|\frac{\mathbf{e}}{\|\mathbf{e}\|_p} \otimes \mathbf{e}\|_p = \|\frac{\mathbf{e}^2}{\|\mathbf{e}\|_p}\|_p = \frac{\|\mathbf{e}^2\|_p}{\|\mathbf{e}\|_p} \tag{4}$$

In practice, the elements of embedding vectors are much less than 1 in most cases. Therefore, the maximum change $\|\mathbf{e}^2\|_p/\|\mathbf{e}\|_p$ is significantly lower than the unrestricted scale change in SFBR.

Extension of RSCF The shared affine transformation can be easily extended to $Linear-2$ introduced in SFBR by extending shared affine transformation $\mathbf{W_e} \in \mathbf{R}^{n \times n}$ to $\mathbf{W_e} \in \mathbf{R}^{n \times 2n}$. RSCF (Linear-2) can be written as:

$$\mathbf{W_r}^{\text{Linear-2}} = \begin{bmatrix} diag(\mathbf{w}_1) & diag(\mathbf{w}_2) \\ diag(\mathbf{w}_3) & diag(\mathbf{w}_4) \end{bmatrix} \quad (5)$$

where $\mathbf{W_r}^{\text{Linear-2}}, \in \mathbf{R}^{n \times n}$ is ET built from the relation-specific change vector $\mathbf{N}_p(\mathbf{rA}) + 1$ of RSCF that is notated as concatenation of diagonal values of $\mathbf{w}_1, \mathbf{w}_2, \mathbf{w}_3, \mathbf{w}_4 \in \mathbf{R}^{n/2}$. Following the setting of SFBR, RSCF (Linear-2) and RSCF are applied to both head and tail entities in DBM, and RSCF is applied to the only head entity in TDM. Examples of RSCF for different models are given in Appendix A

4 Related Works

Disconnection of Relation-Specific Transformation in ETM ETM is a model that uses relation-specific ET to model various attributes of an entity. Models such as TransH (Wang et al., 2014), TransR (Lin et al., 2015), and TransD (Ji et al., 2015) are variants of TransE (Bordes et al., 2013), designed to handle complex relations by employing hyperplanes, projection matrices, and dynamic mapping matrices for their transformation functions, respectively. To address the heterogeneity and imbalance presented in TransE and its variants, TransSparse (Ji et al., 2016) utilizes adaptive sparse matrices to model different types of relations. PairRE (Chao et al., 2021) performs a scaling operations through the Hadamard product to the head and tail entities. SFBR (Liang et al., 2021) presents a universal entity transformation-based model applicable to both DBM and TDM. To handle complex relation in TDM, STaR (Li and Yang, 2022) integrates scaling, translation, and rotation operation for semantic matching scoring functions. ReflectE (Zhang et al., 2022a) models the transformation function using relation-specific dynamic reflection hyperplanes. CompoundE (Ge et al., 2023) applied compound operation to both head and tail entities. However, these models have no chance for inductive bias sharing due to the separate parameter of ET. Moreover, except for the SFBR, these models only use DBM or TDM.

Entity Embedding Concentration in ETM SFBR (Liang et al., 2021) applies ET to both DBM and TDM. However, it also suffers from inductive bias loss due to the separate parameter of ET and indistinguishable score distribution because of the entity embedding concentration.

Dataset	Entities	Relations	Triples		
			Train	Valid	Test
WN18RR	40,943	11	86,835	3,034	3,134
FB15k-237	14,541	237	272,115	17,535	20,466
YAGO3-10	123,182	37	1,079,040	5,000	5,000

Table 1: Statistics of KGC Benchmark Datasets

5 Experiments

5.1 Settings

Dataset To evaluate our proposed RSCF models, we consider three KGs datasets: WN18RR (Toutanova and Chen, 2015), FB15k-237 (Dettmers et al., 2018), and YAGO3-10 (Mahdisoltani et al., 2013) The statistics for the three benchmark datasets are as shown in Table 1

Evaluation Protocol We evaluated the performance of KGC following the filtered setting (Bordes et al., 2013). The filtered setting removes all valid triples from the candidate set when evaluating the test set, except for the predicted test triple. We adopt the MRR and Hits@N to compare the performance of different KGE models. MRR is the average of the inverse mean rank of the entities and Hits@N is the proportion of correct entities ranked within top k.

Baselines and Training Protocol We compare the performance of RSCF with the two categories of KGE models: 1) DBM with entity transformation including TransH (Wang et al., 2014), TransR (Lin et al., 2015), TransD (Ji et al., 2015), PairRE (Chao et al., 2021), SFBR (Liang et al., 2021), ReflectE (Zhang et al., 2022a) and CompoundE (Ge et al., 2023), 2) TDM with entity transformation including STaR (Li and Yang, 2022), SFBR (Liang et al., 2021) and SFBR with Normalization (SFBR (N)[2]). Because RSCF is a module that is plugged in based on existing models, we used DBM, including TransE, RotatE, and TDM, including CP, RESCAL, and ComplEX as base models.

5.2 Performance

Performance on Distance-Based Model Table 2 shows the comparison of the performance of the RSCF model and DBMs with ET on WN18RR and FB15k-237. In filter-based models, RSCF shows similar or higher performance than SFBR in most

[2]Detailed description of SFBR (N) is given in Appendix B

Distance-Based Model with Entity Transformation	WN18RR			FB15k-237		
	MRR	H@1	H@10	MRR	H@1	H@10
Non Filter Based Models						
TransH (Wang et al., 2014) †	.220	.042	.495	.299	.201	.488
TransR (Lin et al., 2015) †	.219	.050	.498	.309	.220	.489
TransD (Ji et al., 2015) †	.211	.087	.505	.306	.218	.486
PairRE (Chao et al., 2021)	-	-	-	.351	.256	.544
ReflectE (Zhang et al., 2022a)	.488	.450	.559	.358	.263	.546
CompoundE (Ge et al., 2023)	.491	.450	.576	.357	.264	.545
Filter Based Models						
TransE-SFBR (Diag) (Liang et al., 2021)	.242	.028	.548	.338	.240	.538
TransE-RSCF (Ours)	.242	.030	.550	.349	.250	.549
TransE-SFBR (Linear-2) (Liang et al., 2021)	.263	.110	.495	.354	.258	.545
TransE-RSCF (Linear-2) (Ours)	.301	.187	.512	.356	.260	.546
RotatE-SFBR (Diag) (Liang et al., 2021)	.489	.437	**.593**	.351	.254	.549
RotatE-RSCF (Ours)	.489	.441	.584	.355	.259	.548
RotatE-SFBR (Linear-2) (Liang et al., 2021)	.490	.447	.576	.355	.258	**.553**
RotatE-RSCF (Linear-2) (Ours)	**.496**	**.455**	.581	**.361**	**.267**	.551

Table 2: Test performance of DBM-based KGC on FB15k-237 and WN18RR. Bold indicates the best result, underlined signifies the second best result, and red denotes performance improvement over SFBR. (†: reproduced result from Zhang et al. (2020a)).

Tensor Decomposition Model with Eentity Transformation	WN18RR			FB15k-237			YAGO3-10		
	MRR	H@1	H@10	MRR	H@1	H@10	MRR	H@1	H@10
Non Filter Based Models									
STaR-DURA (Li and Yang, 2022)	.497	.452	**.583**	.368	.273	.557	.585	.513	.713
Filter Based Models									
CP-DURA + SFBR †	.479	.441	.555	.368	.275	.557	.581	.510	.707
CP-DURA + SFBR (N)	.480	.442	.555	.368	.274	.558	.582	.513	.708
CP-DURA + RSCF (Ours)	.481	.443	.556	.368	.273	.558	.584	.514	.711
RESCAL-DURA + SFBR †	.497	.454	.576	.369	.277	.550	.578	.503	.712
RESCAL-DURA + SFBR (N)	**.499**	.457	.577	.369	.277	.552	.581	.510	.710
RESCAL-DURA + RSCF (Ours)	**.499**	**.459**	.578	.369	.277	.552	.581	.509	.714
ComplEX-DURA + SFBR †	.491	.450	.571	.373	.277	.563	.587	.517	.715
ComplEX-DURA + SFBR (N)	.493	.452	.572	.374	.278	.564	.586	.514	**.717**
ComplEX-DURA + RSCF (Ours)	.497	.454	.581	**.375**	**.279**	**.565**	**.589**	**.518**	**.717**

Table 3: Test performance of TDM-based KGC on FB15k-237, WN18RR, and YAGO3-10. Bold indicates the best result, underlined signifies the second best result, and red denotes performance improvement over SFBR. (SFBR (N): SFBR with normalization, †: reproduced results whose reference results in Appendix E).

settings. Even in comparison with the non-filtered model, the best filtered model (RotatE-RSCF) significantly outperforms CompoundE, the state-of-the-art DBM method.

Performance on Tensor Decomposition Model Table 3 shows performance of TDMs. In filter-based models, our model shows performance improvements in almost all datasets. On WN18RR, RESCAL-RSCF shows the highest performance, outperforming the SFBR. On FB15k-237 and YAGO3-10, ComplEX-DURA-RSCF shows the highest performance, outperforming the SFBR. Furthermore, in performance comparison with the non-filtered model, ComplEX-DURA-RSCF outperforms STaR on FB15k-237 and YAGO3-10.

Ablation Study In Table 3, applying only normalization to SFBR slightly improves performance on overall datasets and base models, but using affine transformation of RSCF shows more significant results.

Relation-Wise Performance for Long Tailed Distribution To demonstrate the effectiveness of our model on long-tail relations, we sorted relations by their frequency in the train set and divided them into ten groups. Each group has the same relation number. Table 4 shows the MRR scores for each group in TransE, TransE-RSCF (RSCF) and TransE-SFBR (Diag) (SFBR). The results showed that RSCF outperformed SFBR and TrasnE in all groups, indicating that RSCF is also effective for

Relation Set	Frequency	TransE MRR	RSCF MRR	SFBR MRR
Set1	2435	0.489	**0.518**	0.486
Set2	5657	0.510	**0.534**	0.521
Set3	9832	0.403	**0.441**	0.420
Set4	15410	0.463	**0.475**	0.465
Set5	23209	0.326	**0.337**	0.336
Set6	34192	0.509	**0.521**	0.520
Set7	50157	0.371	**0.379**	0.371
Set8	74067	0.463	**0.482**	0.474
Set9	128284	0.311	**0.329**	0.314
Set10	272115	0.346	**0.366**	0.355

Table 4: KGC performance of each 10% of unique relations sorted by their frequency in a long-tailed distribution.

long-tail relations.

Performance on Semantically Distinguished Relation Groups Table 5 presents the validation MRR for each relation group, defined as preliminary results in Figure 1. RSCF outperformed SFBR in all groups except for the position group. These results show that reflecting the relation semantics into the transformation function can improve model performance.

Relation Group	TransE MRR	RSCF MRR	SFBR MRR
position	0.370	0.395	**0.409**
currency	**0.529**	0.522	0.518
film production	0.218	**0.247**	0.224
film actor	0.128	**0.139**	0.133
people place	0.276	**0.287**	0.283
film place	0.293	**0.323**	0.314
music role	0.168	**0.176**	0.154
orgaziation place	0.591	**0.626**	0.618
producer type	**0.397**	0.395	0.381
award category	0.353	**0.392**	0.369

Table 5: KGC performance of each relation-semantic group on the FB15k-237

Qualitative Example Analysis Table 6 presents the correct answers for three sample queries, along with the related triples in the training set, and the ranks obtained by TransE-RSCF and TransE-SFBR (Diag). Since relations of the sampled queries belong to the people place group used in Figure.1, the related triples represent triples that include relations belonging to the people place group. In Table 6, RSCF shows enhanced performance compared to SFBR, indicating that RSCF can use trained bias between similar relations.

5.3 In-Depth Analysis

Relation-Semantics Consistency of Entity Embedding We selected eight queries $(h, r, ?)$ in FB15k-237. Each query has more than 50 answers and has different relation. Figure 4 shows the embeddings of the related tail entities of queries generated by TransE-SFBR (Diag) (a) and TransE-RSCF (b). This figure illustrates that RSCF concentrates entity embeddings in the same relation group and decouples embeddings in different groups compared to SFBR. The result implies that the relation-specific separation of entity embeddings properly works as SFBR, but it also maintains the relation-semantics consistency. See more details about the eight queries in Appendix G.

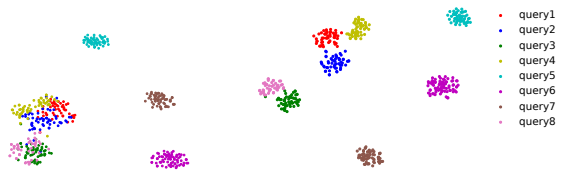

(a) SFBR (b) RSCF

Figure 4: Visualization for tail entity embeddings for the same queries.

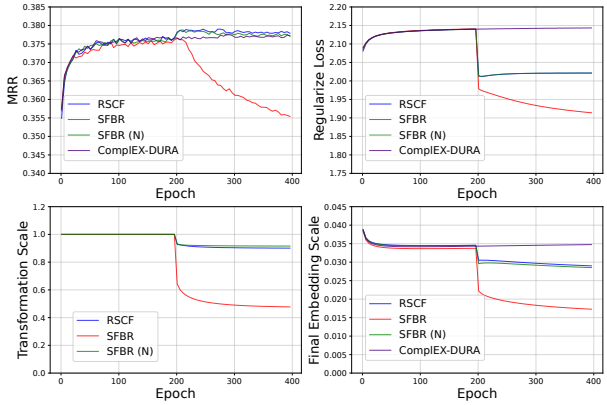

Figure 5: MRR, regularization loss, entity transformation scale, and final entity embedding scale over epochs on the FB15k-237.

Embedding Scale and Score Distribution Recovery Figure 5 presents the MRR, regularize loss, transformation scale, and final entity embedding scale over epochs in the validation set of FB15k-237. Following the approach of SFBR (Liang et al., 2021), we applied the only DURA regularizer up to 200 epochs in ComplEX, then RSCF, SFBR, and SFBR (N) are plugged in after 200 epochs. In the results, SFBR shows a decrease in both transformation scale and final entity embedding scale, accompanied by a steady decrease in the regularizer loss. In contrast, RSCF and SFBR (N) show almost no

Query (h, r, ?) | Correct Answer	Related Triples in Training Set	Rank(R/S)
(Guillermo del Toro, /people/person/place_of_birth, ?) | Guadalajara	(Guillermo del Toro, /people/person/places_lived./people/place_lived/location, Jalisco) (Guillermo del Toro, /people/person/nationality, Mexico)	**9** / 35
(Shawn Pyfrom, /people/person/places_lived./people/place_lived/location, ?) | Florida	(Shawn Pyfrom, /people/person/place_of_birth, Tampa) (Shawn Pyfrom, /people/person/nationality, United States of America)	**5** / 32
(Walt Whitman, /people/person/places_lived./people/place_lived/location, ?) | New York	(Walt Whitman, /people/deceased_person/place_of_death, Camden) (Walt Whitman, /people/person/nationality, United States of America)	**3** / 21

Table 6: Example KGC results of RSCF compared to SFBR (R: rank of RSCF, S: rank of SFBR). Related triples show that similar relations to the queries have similar entities to the correct answers in the training set.

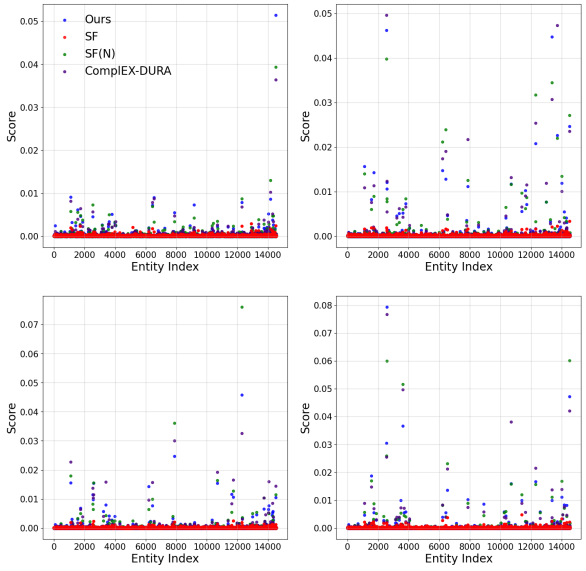

Figure 6: Score-entity graph for randomly samples queries from Figure 6

decrease in the transformation scale, and the final entity embedding scale is maintained. Also, the regularizer loss converged at a certain point, indicating that both RSCF and SFBR (N) can maintain the embedding scale due to normalization. Furthermore, the MRR decreases in SFBR, while it increases in both RSCF and SFBR (N). This result implies that entity embedding concentration negatively affects to model performance.

To investigate the detailed change of score distribution that directly affects performance, we randomly sample four queries and present the score distribution for all tail entities as shown in Figure 6. In the results, SFBR shows near zero scores for most entities, and distributions for the queries are significantly similar. Applying normalization or RSCF, the diversity of scores is recovered as the original base model.

Impact on Over-Smoothed Queries To assess the impact of indistinguishable score distribution, we conducted a performance evaluation for a selected relation to show critical entity embedding concentration in Figure 2. Table 7 presents the validation performance for all queries associated with the selected relation. SFBR shows significantly lower performance than RSCF, SFBR (N), and the ComplEX-DURA. This result implies that indistinguishable score distribution strongly affects to the accurate prediction of SFBR, simply applying normalization and RSCF gradually recovers it.

Model	MRR	H@1	H@10
ComplEX-DURA + RSCF	**.395**	**.283**	**.609**
ComplEX-DURA + SFBR	.267	.152	.522
ComplEX-DURA + SFBR (N)	.366	.239	.587
ComplEX-DURA	.347	.217	.609

Table 7: KGC performance of queries to cause strong entity embedding concentration in SFBR.

6 Conclusion

In this paper, we address the limit in inducing relation-semantics consistency, implying that semantically similar relations have similar entity transformation, on entity transformation models for KGC, especially SFBR. We clarify two causes, disconnected entity transformation representation and entity embedding concentration, and provide a novel relation-semantics consistent filter (RSCF) method using shared affine transform to generate the change of entity embedding, normalize it and add it to the embedding. This method significantly improves the performance of KGC compared to state-of-the-art KGE methods for overall relations and especially rare relations.

7 Limitations and Future Works

RSCF uses the simplest form of affine transformation, but it has a limit of expressing all changes across all embeddings, which requires more advanced approach. Future work should extend the method to additional KGE models to enhance generality.

References

Antoine Bordes, Nicolas Usunier, Alberto Garcia-Duran, Jason Weston, and Oksana Yakhnenko.

2013. Translating embeddings for modeling multi-relational data. *Advances in neural information processing systems*, 26.

Yixin Cao, Xiang Wang, Xiangnan He, Zikun Hu, and Tat-Seng Chua. 2019. Unifying knowledge graph learning and recommendation: Towards a better understanding of user preferences. In *The world wide web conference*, pages 151–161.

Ines Chami, Adva Wolf, Da-Cheng Juan, Frederic Sala, Sujith Ravi, and Christopher Ré. 2020. Low-dimensional hyperbolic knowledge graph embeddings. *arXiv preprint arXiv:2005.00545*.

Linlin Chao, Jianshan He, Taifeng Wang, and Wei Chu. 2021. Pairre: Knowledge graph embeddings via paired relation vectors. In *Proceedings of the 59th Annual Meeting of the Association for Computational Linguistics and the 11th International Joint Conference on Natural Language Processing (Volume 1: Long Papers)*, pages 4360–4369.

Tim Dettmers, Pasquale Minervini, Pontus Stenetorp, and Sebastian Riedel. 2018. Convolutional 2d knowledge graph embeddings. In *Proceedings of the AAAI conference on artificial intelligence*, volume 32.

Xin Dong, Evgeniy Gabrilovich, Geremy Heitz, Wilko Horn, Ni Lao, Kevin Murphy, Thomas Strohmann, Shaohua Sun, and Wei Zhang. 2014. Knowledge vault: A web-scale approach to probabilistic knowledge fusion. In *Proceedings of the 20th ACM SIGKDD international conference on Knowledge discovery and data mining*, pages 601–610.

Yuan Fang, Kingsley Kuan, Jie Lin, Cheston Tan, and Vijay Chandrasekhar. 2017. Object detection meets knowledge graphs. International Joint Conferences on Artificial Intelligence.

Junyu Gao, Tianzhu Zhang, and Changsheng Xu. 2019. I know the relationships: Zero-shot action recognition via two-stream graph convolutional networks and knowledge graphs. In *Proceedings of the AAAI conference on artificial intelligence*, volume 33, pages 8303–8311.

Xiou Ge, Yun Cheng Wang, Bin Wang, and C-C Jay Kuo. 2023. Compounding geometric operations for knowledge graph completion. In *Proceedings of the 61st Annual Meeting of the Association for Computational Linguistics (Volume 1: Long Papers)*, pages 6947–6965.

Shijie Geng, Zuohui Fu, Juntao Tan, Yingqiang Ge, Gerard De Melo, and Yongfeng Zhang. 2022. Path language modeling over knowledge graphsfor explainable recommendation. In *Proceedings of the ACM Web Conference 2022*, pages 946–955.

Cosimo Gregucci, Mojtaba Nayyeri, Daniel Hernández, and Steffen Staab. 2023. Link prediction with attention applied on multiple knowledge graph embedding models. In *Proceedings of the ACM Web Conference 2023*, pages 2600–2610.

Guoliang Ji, Shizhu He, Liheng Xu, Kang Liu, and Jun Zhao. 2015. Knowledge graph embedding via dynamic mapping matrix. In *Proceedings of the 53rd annual meeting of the association for computational linguistics and the 7th international joint conference on natural language processing (volume 1: Long papers)*, pages 687–696.

Guoliang Ji, Kang Liu, Shizhu He, and Jun Zhao. 2016. Knowledge graph completion with adaptive sparse transfer matrix. In *Proceedings of the AAAI Conference on Artificial Intelligence*, volume 30.

Timothée Lacroix, Nicolas Usunier, and Guillaume Obozinski. 2018. Canonical tensor decomposition for knowledge base completion. In *International Conference on Machine Learning*, pages 2863–2872. PMLR.

Jiayi Li and Yujiu Yang. 2022. Star: Knowledge graph embedding by scaling, translation and rotation. In *International Conference on AI and Mobile Services*, pages 31–45. Springer.

Zongwei Liang, Junan Yang, Hui Liu, and Keju Huang. 2021. A semantic filter based on relations for knowledge graph completion. In *Proceedings of the 2021 Conference on Empirical Methods in Natural Language Processing*, pages 7920–7929.

Yankai Lin, Zhiyuan Liu, Maosong Sun, Yang Liu, and Xuan Zhu. 2015. Learning entity and relation embeddings for knowledge graph completion. In *Proceedings of the AAAI conference on artificial intelligence*, volume 29.

Ye Liu, Yao Wan, Lifang He, Hao Peng, and S Yu Philip. 2021. Kg-bart: Knowledge graph-augmented bart for generative commonsense reasoning. In *Proceedings of the AAAI Conference on Artificial Intelligence*, volume 35, pages 6418–6425.

Farzaneh Mahdisoltani, Joanna Biega, and Fabian M Suchanek. 2013. Yago3: A knowledge base from multilingual wikipedias. In *CIDR*.

Mojtaba Nayyeri, Chengjin Xu, Franca Hoffmann, Mirza Mohtashim Alam, Jens Lehmann, and Sahar Vahdati. 2021. Knowledge graph representation learning using ordinary differential equations. In *Proceedings of the 2021 Conference on Empirical Methods in Natural Language Processing*, pages 9529–9548.

Guanglin Niu, Bo Li, Yongfei Zhang, and Shiliang Pu. 2022. Cake: A scalable commonsense-aware framework for multi-view knowledge graph completion. *arXiv preprint arXiv:2202.13785*.

Aleksandar Pavlović and Emanuel Sallinger. 2022. Expressive: A spatio-functional embedding for knowledge graph completion. In *The Eleventh International Conference on Learning Representations*.

Zhiqing Sun, Zhi-Hong Deng, Jian-Yun Nie, and Jian Tang. 2019. Rotate: Knowledge graph embedding by relational rotation in complex space. *arXiv preprint arXiv:1902.10197*.

Kristina Toutanova and Danqi Chen. 2015. Observed versus latent features for knowledge base and text inference. In *Proceedings of the 3rd workshop on continuous vector space models and their compositionality*, pages 57–66.

Théo Trouillon, Johannes Welbl, Sebastian Riedel, Éric Gaussier, and Guillaume Bouchard. 2016. Complex embeddings for simple link prediction. In *International conference on machine learning*, pages 2071–2080. PMLR.

Hongwei Wang, Fuzheng Zhang, Miao Zhao, Wenjie Li, Xing Xie, and Minyi Guo. 2019. Multi-task feature learning for knowledge graph enhanced recommendation. In *The world wide web conference*, pages 2000–2010.

Zhen Wang, Jianwen Zhang, Jianlin Feng, and Zheng Chen. 2014. Knowledge graph embedding by translating on hyperplanes. In *Proceedings of the AAAI conference on artificial intelligence*, volume 28.

Bishan Yang, Wen-tau Yih, Xiaodong He, Jianfeng Gao, and Li Deng. 2014. Embedding entities and relations for learning and inference in knowledge bases. *arXiv preprint arXiv:1412.6575*.

Jinfa Yang, Xianghua Ying, Yongjie Shi, Xin Tong, Ruibin Wang, Taiyan Chen, and Bowei Xing. 2022. Knowledge graph embedding by adaptive limit scoring loss using dynamic weighting strategy. In *Findings of the Association for Computational Linguistics: ACL 2022*, pages 1153–1163.

Qianjin Zhang, Ronggui Wang, Juan Yang, and Lixia Xue. 2022a. Knowledge graph embedding by reflection transformation. *Knowledge-Based Systems*, 238:107861.

Siheng Zhang, Zhengya Sun, and Wensheng Zhang. 2020a. Improve the translational distance models for knowledge graph embedding. *Journal of Intelligent Information Systems*, 55:445–467.

Wenqian Zhang, Shangbin Feng, Zilong Chen, Zhenyu Lei, Jundong Li, and Minnan Luo. 2022b. Kcd: Knowledge walks and textual cues enhanced political perspective detection in news media. *arXiv preprint arXiv:2204.04046*.

Yongqi Zhang, Zhanke Zhou, Quanming Yao, and Yong Li. 2022c. Efficient hyper-parameter search for knowledge graph embedding. In *Proceedings of the 60th Annual Meeting of the Association for Computational Linguistics (Volume 1: Long Papers)*, pages 2715–2735.

Zhanqiu Zhang, Jianyu Cai, and Jie Wang. 2020b. Duality-induced regularizer for tensor factorization based knowledge graph completion. *Advances in Neural Information Processing Systems*, 33:21604–21615.

Yucheng Zhou, Xiubo Geng, Tao Shen, Guodong Long, and Daxin Jiang. 2022. Eventbert: A pre-trained model for event correlation reasoning. In *Proceedings of the ACM Web Conference 2022*, pages 850–859.

A Special Cases with RSCF

Let $\mathbf{h_r}$, $\mathbf{t_r}$ are transformed head and tail embedding by RSCF, then the score function $d_r(\mathbf{h}, \mathbf{r})$ of TransE-RSCF can be expressed as:

$$d_r(\mathbf{h}, \mathbf{r}) = \|\mathbf{h_r} + \mathbf{r} - \mathbf{t_r}\| \tag{6}$$

The score function $d_r(\mathbf{h}, \mathbf{r})$ of RotatE-RSCF can be expressed as:

$$d_r(\mathbf{h}, \mathbf{r}) = \|\mathbf{h_r} \circ \mathbf{r} - \mathbf{t_r}\| \tag{7}$$

The score function $d_r(\mathbf{h}, \mathbf{r})$ of RESCAL-RSCF can be expressed as:

$$d_r(\mathbf{h}, \mathbf{r}) = \|\mathbf{h_r r t}\| \tag{8}$$

In TDM, tail embeddings are not transformed according to the settings of SFBR in order to reduce computational costs.

B SFBR with Normalization

Let $\mathbf{W_r}$ is relation-specific ET using separate parameters, then SFBR with normalization can be written as:

$$\mathbf{N}_p(\mathbf{W_r}) + 1 \tag{9}$$

where $\mathrm{N}_p(\mathbf{W_r}) = \frac{\mathbf{W_r}}{\|\mathbf{W_r}\|_p}$. Additionally, transformed entity embedding can be described as:

$$\mathbf{e_r} = (\mathbf{N}_p(\mathbf{W_r}) + 1)\mathbf{e} \tag{10}$$

where $\mathbf{e}$ is a original entity embedding.

C Proof of Consistency of Normalized Change

For any relation embedding r_1, r_2, r_3 on a line and their mapped ET T_1, T_2, T_3 by an affine transform, then the consistency holds. Let T_2 is on $\overline{T_1T_3}$, and $\overline{r_1r_2}$ is shorter $\overline{r_2r_3}$. Then, $\overline{T_1T_2} < \overline{T_2T_3}$ by the properties of affine transformation. Because T_2 is an interpolated point of T_1 and T_3, $\angle T_1OT_2 < \angle T_2OT_3$. After normalization, let ETs projected on T_1', T_2', and T_3'. $\overline{T_1'T_2'} = \sqrt{2 - 2\cos\angle T_1'OT_2'}$, and $\overline{T_2'T_3'} = \sqrt{2 - 2\cos\angle T_2'OT_3'}$ by simple cosine rule. Cosine function is monotonically decreasing for angles less than π. Therefore, $\overline{T_1'T_2'} < \overline{T_2'T_3'}$

Embedding based Model	WN18RR			FB15k-237		
	MRR	H@1	H@10	MRR	H@1	H@10
TransE (Bordes et al., 2013)	.226	-	.501	.294	-	.465
DistMult (Yang et al., 2014)	.430	.390	.490	.241	.155	.419
ComplEX (Trouillon et al., 2016)	.440	.410	.510	.247	.158	.428
RotatE (Sun et al., 2019)	.476	.428	.571	.338	.241	.533
ROTH (Chami et al., 2020)	.496	.449	.586	.348	.252	.540
ComplEX-DURA (Zhang et al., 2020b)	.491	.449	.571	.371	.276	.560
FieldE (Nayyeri et al., 2021)	.48	.44	.57	.36	.27	.55
KGTuner (Zhang et al., 2022c)	.484	.440	.562	.352	.263	.530
RotatE-IAS (Yang et al., 2022)	.483	**.467**	.570	.339	.242	.532
CAKE (Niu et al., 2022)	-	-	-	.321	.227	.515
STaR-DURA (Li and Yang, 2022)	.497	.452	.583	.368	.273	.557
ExpressivE (Pavlović and Sallinger, 2022)	.482	.407	**.619**	.350	.256	.535
SEPA (Gregucci et al., 2023)	**.500**	.454	.591	.360	.264	.549
CompoundE (Ge et al., 2023)	.491	.450	.576	.357	.264	.545
ComplEX-DURA + RSCF (Ours)	.497	.454	.581	**.375**	**.279**	**.565**

Table 8: Test performance in broader approaches with different constraints based on embedding based KGC on FB15k-237 and WN18RR. Bold indicates the best result, and underline indicates the second best result.

Tensor Decomposition Model	WN18RR			FB15k-237			YAGO3-10		
	MRR	H@1	H@10	MRR	H@1	H@10	MRR	H@1	H@10
CP-DURA + SFBR(R)	.479	.441	.555	.368	**.275**	.557	.581	**.510**	.707
CP-DURA + SFBR (Liang et al., 2021)	**.485**	**.447**	**.561**	**.370**	.274	**.563**	**.582**	**.510**	**.711**
RESCAL-DURA + SFBR(R)	.497	.454	.576	**.369**	.277	.550	.578	.503	.712
RESCAL-DURA + SFBR (Liang et al., 2021)	**.500**	**.458**	**.581**	**.369**	**.276**	**.555**	**.581**	**.509**	**.712**
ComplEX-DURA + SFBR(R)	.491	.450	.571	.373	**.277**	.563	**.587**	**.517**	**.715**
ComplEX-DURA + SFBR (Liang et al., 2021)	**.498**	**.454**	**.584**	**.374**	**.277**	**.567**	.584	.512	.712

Table 9: Comparison of reproduced SFBR and SFBR reported in Liang et al. (2021)

D Performance Comparison of RSCF with Other Knowledge Graph Embedding Models

Table 8 shows the comparison of the test performance of the RSCF and embedding based model on WN18RR and FB15k-237. ComplEX-DURA + RSCF outperforms all other models in FB15k-237, and shows competitive results in WN18RR.

E Reproduce of SFBR in TDM

We attempted to reproduce SFBR. During the reproduction process, we designed and executed the experiments based on the information provided in the SFBR and the publicly available datasets. Furthermore, in an attempt to clarify unclear aspects, we tried to communicate with the authors through multiple emails. However, the performance reported in the paper was not achieved. Table 9 shows reproduced SFBR and SFBR that is reported in Liang et al. (2021).

F Implementation Details

We found that the performance of TransE-RSCF on WN18RR is sensitive to the warm-up step. Therefore, we excluded the warm-up step when training TransE-RSCF on WN18RR. Other hyperparameters are consistent with the hyperparameters in Sun et al. (2019). Additionally, when training the TDM, we followed the experimental settings described in the SFBR (Liang et al., 2021). The presented results of RSCF represent the best performance among five runs for each model. Experiments for the DBM were conducted on an NVIDIA RTX 8000 GPU with 48GB of memory, while experiments for the TDM were conducted on an NVIDIA 2080TI with 11GB.

G Queries in Relation-Specific Separation of Entity Embedding

Table 10 presents the eight queries used in Relation-Specific Separation of Entity Embedding (Section 5.3). Note that a query consists of $(h, r, ?)$, where

Index	Query
1	(Cancer, /people/cause_of_death/people', ?)
2	(Rock and roll, /music/genre/artists, ?)
3	(Academy Award for Best Actor, /award/award_category/winners./award/award_honor/award_winner, ?)
4	(Bachelor of Science, /education/educational_degree/people_with_this_degree./education/education/major_field_of_study, ?)
5	(Football, /sports/sport/pro_athletes./sports/pro_sports_played/athlete, ?)
6	(MCA Records, /music/record_label/artist, ?)
7	(Yale University, /education/educational_institution/students_graduates./education/education/student, ?)
8	(National Society of Film Critics Award for Best Director, /award/award_category/nominees./award/award_nomination/nominated_for, ?)

Table 10: The queries in T-SNE visualizations that are used in Figure 4

h, r denote head entity and relation, respectively.

H Relation Groups for Entity Transformation

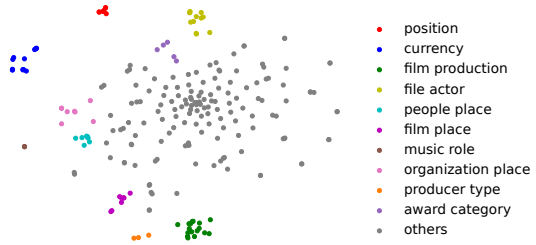

Figure 7: Visualization of relation embeddings of TransE using T-SNE

Figure 7 illustrates the relation embedding of TransE. We select ten relation groups whose relation embeddings build clear and mutually decoupled clusters, which implies semantically distinguished relation groups. The other relations are plotted as grey points. The relations corresponding to each group are listed in Table 11. Note that similar relations belong to the same group.

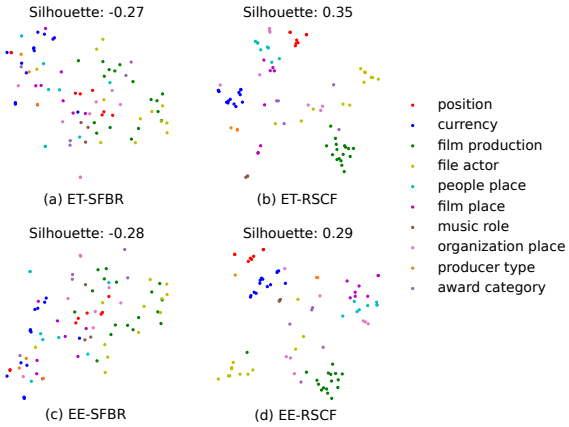

Figure 8: Tail entity-transformations and entity embeddings for semantically similar relation groups. (a) and (b) indicate ET of SFBR and RSCF, (c) and (d) indicate EE of SFBR and RSCF.

I Distribution of Tail Entity-Transformations and Corresponding Entity Embedding

Figure 8 presents the T-SNE visualization of tail entity-transformations and corresponding entity embeddings. Even in the tail, RSCF shows more in-cluster concentration and decoupling clusters. Also RSCF exhibits higher silhouette scores compared to SFBR.

Relation Group	Relations
position	/sports/sports_team/roster./basketball/basketball_roster_position/position
	/soccer/football_team/current_roster./soccer/football_roster_position/position
	/ice_hockey/hockey_team/current_roster./sports/sports_team_roster/position
	/sports/sports_team/roster./american_football/football_historical_roster_position/position_s
	/sports/sports_team/roster./baseball/baseball_roster_position/position
	/sports/sports_team/roster./american_football/football_roster_position/position
	/american_football/football_team/current_roster./sports/sports_team_roster/position
	/soccer/football_team/current_roster./sports/sports_team_roster/position
currency	/location/statistical_region/gdp_nominal_per_capita./measurement_unit/dated_money_value/currency
	/film/film/estimated_budget./measurement_unit/dated_money_value/currency
	/business/business_operation/operating_income./measurement_unit/dated_money_value/currency
	/organization/endowed_organization/endowment./measurement_unit/dated_money_value/currency
	/business/business_operation/revenue./measurement_unit/dated_money_value/currency
	/business/business_operation/assets./measurement_unit/dated_money_value/currency
	/location/statistical_region/rent50_2./measurement_unit/dated_money_value/currency
	/education/university/local_tuition./measurement_unit/dated_money_value/currency
	/location/statistical_region/gdp_real./measurement_unit/adjusted_money_value/adjustment_currency
	/education/university/domestic_tuition./measurement_unit/dated_money_value/currency
	/education/university/international_tuition./measurement_unit/dated_money_value/currency
	/location/statistical_region/gdp_nominal./measurement_unit/dated_money_value/currency
	/location/statistical_region/gni_per_capita_in_ppp_dollars./measurement_unit/dated_money_value/currency
	/base/schemastaging/person_extra/net_worth./measurement_unit/dated_money_value/currency
film production	/film/film/costume_design_by
	/film/film/executive_produced_by
	/award/award_winning_work/awards_won./award/award_honor/award_winner
	/tv/tv_program/program_creator
	/film/film/film_art_direction_by
	/film/film/music
	/film/film/film_production_design_by
	/film/film/other_crew./film/film_crew_gig/crewmember
	/film/film/produced_by
	/tv/tv_program/regular_cast./tv/regular_tv_appearance/actor
	/film/film/edited_by
	/film/film/written_by
	/film/film/personal_appearances./film/personal_film_appearance/person
	/film/film/story_by
	/film/film/cinematography
	/film/film/dubbing_performances./film/dubbing_performance/actor
	/film/film/production_companies
file actor	/award/award_nominee/award_nominations./award/award_nomination/nominated_for
	/tv/tv_network/programs./tv/tv_network_duration/program
	/film/special_film_performance_type/film_performance_type./film/performance/film
	/film/director/film
	/tv/tv_personality/tv_regular_appearances./tv/tv_regular_personal_appearance/program
	/film/film_set_designer/film_sets_designed
	/tv/tv_writer/tv_programs./tv/tv_program_writer_relationship/tv_program
	/film/actor/film./film/performance/film
	/tv/tv_producer/programs_produced./tv/tv_producer_term/program
	/media_common/netflix_genre/titles
	/film/film_distributor/films_distributed./film/film_film_distributor_relationship/film

	/film/film_subject/films
people place	/music/artist/origin
	/people/person/places_lived./people/place_lived/location
	/people/person/place_of_birth
	/government/politician/government_positions_held./government/government_position_held/jurisdiction_of_office
	/people/deceased_person/place_of_death
	/people/person/nationality
	/people/deceased_person/place_of_burial
	/people/person/spouse_s./people/marriage/location_of_ceremony
film place	/film/film/distributors./film/film_film_distributor_relationship/region
	/film/film/featured_film_locations
	/film/film/release_date_s./film/film_regional_release_date/film_release_region
	/film/film/release_date_s./film/film_regional_release_date/film_regional_debut_venue
	/film/film/country
	/film/film/runtime./film/film_cut/film_release_region
	/tv/tv_program/country_of_origin
	/film/film/film_festivals
music role	/music/group_member/membership./music/group_membership/role
	/music/artist/track_contributions./music/track_contribution/role
	/music/artist/contribution./music/recording_contribution/performance_role
organization place	/organization/organization/headquarters./location/mailing_address/state_province_region
	/organization/organization/place_founded
	/user/ktrueman/default_domain/international_organization/member_states
	/organization/organization/headquarters./location/mailing_address/country
	/people/marriage_union_type/unions_of_this_type./people/marriage/location_of_ceremony
	/base/schemastaging/organization_extra/phone_number./base/schemastaging/phone_sandbox/service_location
	/government/legislative_session/members./government/government_position_held/district_represented
	/organization/organization/headquarters./location/mailing_address/citytown
producer type	/tv/tv_producer/programs_produced./tv/tv_producer_term/producer_type
	/film/film/other_crew./film/film_crew_gig/film_crew_role
	/tv/tv_program/tv_producer./tv/tv_producer_term/producer_type
award category	/award/award_category/winners./award/award_honor/award_winner
	/award/award_category/winners./award/award_honor/ceremony
	/award/award_category/category_of
	/award/award_category/nominees./award/award_nomination/nominated_for
	/award/award_category/disciplines_or_subjects

Table 11: Clearly distinct relation groups that are selected from original TransE